

# Concentration dependence of superconductivity and the order-disorder transition in the hexagonal rubidium tungsten bronze $\text{Rb}_x\text{WO}_3$ : Interfacial and bulk properties

R. Brusetti,<sup>1</sup> P. Haen,<sup>1</sup> and J. Marcus<sup>2</sup><sup>1</sup>*Centre de Recherches sur les Très Basses Températures, associé à l'Université Joseph Fourier, CNRS, Boîte Postale 166, 38042 Grenoble Cedex 9, France*<sup>2</sup>*Laboratoire d'Etudes des Propriétés Electroniques des Solides, CNRS, Boîte Postale 166, 38042 Grenoble Cedex 9, France*

(Received 10 October 2001; published 4 April 2002)

We revisited the problem of the stability of the superconducting state in  $\text{Rb}_x\text{WO}_3$  and identified the main causes of the contradictory data previously published. We have shown that the ordering of the Rb vacancies in the nonstoichiometric compounds have a major detrimental effect on the superconducting temperature  $T_c$ . The order-disorder transition is of first order only near  $x=0.25$ , where it cannot be quenched effectively and  $T_c$  is reduced below 1 K. We found that the high  $T_c$ 's that were sometimes deduced from resistivity measurements and attributed to compounds with  $0.25 \leq x \leq 0.30$ , are to be ascribed to interfacial superconductivity that generates spectacular nonlinear effects. We also clarified the effect of acid etching and set more precisely the low-rubidium-content boundary of the hexagonal phase. This work makes clear that  $T_c$  would increase continuously (from  $\approx 2$  K up to  $\approx 5.5$  K) as we approach this boundary ( $x \approx 0.20$ ), if no ordering would take place—as it is approximately the case in  $\text{Cs}_x\text{WO}_3$ . This behavior is reminiscent of the tetragonal tungsten bronze  $\text{Na}_x\text{WO}_3$  and asks the same question: what mechanism is responsible for this large increase in  $T_c$  despite the considerable associated reduction of the electron density of state  $\mathcal{D}_{\text{FE}}$ ? By reviewing the other available data on these bronzes we conclude that the theoretical models that are able to answer this question are probably those where the instability of the lattice plays a major role and, particularly, the model that calls upon local structural excitations, associated with the missing alkali atoms.

DOI: 10.1103/PhysRevB.65.144528

PACS number(s): 74.62.-c, 74.70.Dd, 61.50.Nw, 81.30.Hd

## I. INTRODUCTION

Tungsten bronzes with general formula  $M_x\text{WO}_3$  are the first oxides where superconductivity has been observed in 1964.<sup>1</sup> Much attention has been paid to these nonstoichiometric compounds in which it seemed possible to study how the normal and superconducting states react to the filling of the conduction band—as this can be adjusted within rather large ranges by varying the  $M$  content ( $M = \text{alkali}$ ). The most extensive investigations have been carried out on  $\text{Na}_x\text{WO}_3$ —which displays distorted perovskite structures—and particularly on the tetragonal phases, in which a large increase of the superconducting transition temperature  $T_c$  has been observed by reducing the Na content ( $T_c \approx 0.7$  K for  $x=0.4$  whereas  $T_c \approx 3$  K for  $x=0.2$ ).<sup>2</sup> This  $T_c(x)$  dependence was rather puzzling because it seemed quite clear that the density of state at the Fermi level  $\mathcal{D}_{\text{FE}}$  was decreasing with  $x$ . At the same time, an enormous amount of data was accumulated on those properties that are related to the high mobility of the small  $M$  atoms, and which could lead to applications in electrochromic devices and solid electrolytes. These highly mobile  $M$  atoms—and the associated Einstein-like phonon modes—were also suspected to play a determining role in the electron-phonon coupling; however, no clear correlation has been found between the characteristic energy of these modes and the stability of the superconducting state. Many studies have been also devoted to the hexagonal tungsten bronzes (HTB), where higher  $T_c$ 's were obtained,<sup>3</sup> but they yielded many conflicting results, particularly about the  $T_c(x)$  dependence, and this apparently discouraged further attempts to get a better knowledge of these systems. Recently, however, this issue came back in the foreground in-

centally after superconductivity and even high-temperature (superficial) superconductivity was observed in  $\text{WO}_{3-x}$  (Ref. 4) and  $\text{Na}_{0.05}\text{WO}_3$  (Ref. 5), respectively. This encouraged us to revisit the HTB, and particularly  $\text{Rb}_x\text{WO}_3$  where the highest  $T_c$  had been observed.

The structure of these bronzes has been described first by Magnéli.<sup>6</sup> It is based on a framework of  $\text{WO}_6$  (distorted) octahedra that are linked by their corners, as they are in the tetragonal tungsten bronzes, but forming here hexagonal tunnels in which the alkali atoms are accommodated. This structure is stabilized by these atoms if they are large enough (K, Rb, and Cs) and if they fill more than a half of the tunnel sites ( $0.19 \leq x \leq 0.33$ ).

The electronic structure of the tungsten bronzes has been calculated only for cubic  $M\text{WO}_3$  and hexagonal  $\text{WO}_3$  model systems<sup>7</sup> and is rather in good agreement with the results of photoemission measurements carried out on  $\text{Na}_x\text{WO}_3$ .<sup>8</sup> These calculations seem to indicate that the main features of the valence and conduction bands are not very sensitive to the symmetry of the  $\text{WO}_3$  framework and rather independent of  $M$ : the role of the alkali atoms being above all to give their  $s$  electrons to the conduction band whose bottom is mainly built of W  $5d(t_{2g})$  orbitals, hybridized with the O  $2p$ 's.

The hexagonal tunnels running along the  $c$  direction are quite open and this allows the smaller alkali atoms to be very mobile. In the substoichiometric compounds of  $\text{Rb}_x\text{WO}_3$  and  $\text{K}_x\text{WO}_3$ , they tend to order below or near room temperature, respectively.<sup>9,10</sup> According to Sato *et al.*<sup>9</sup> this ordering could be responsible for the drastic reduction of  $T_c$  around  $x \approx 0.25$  and for the electron-transport anomalies observed by Stanley *et al.*<sup>11</sup> and Cadwell *et al.*<sup>12</sup>. Similar but much less

pronounced behaviors were recognized in  $\text{Cs}_x\text{WO}_3$  by Skokan *et al.*,<sup>13</sup> as if the larger size of the Cs atoms impeded their ordering. These authors—belonging to what we shall refer to as the Florida group—also reported an unexplained anisotropy of the upper critical field and Stanley *et al.*<sup>11</sup> underlined the poor reproducibility of their data: some  $\text{Rb}_x\text{WO}_3$  samples displayed large  $T_c$  ( $\approx 7.5$  K) whereas no superconductivity was observed in others belonging to the same composition range. Moreover, other investigations detected no anomaly in the transport properties.<sup>14</sup> Another point was left controversial: acid etching was found to increase the  $T_c$ <sup>15,16</sup> and it was not clear if it was due to a reduction of the Rb content in the bulk or only at the surface of the samples.<sup>17,18</sup> These rather confusing results even led Lefkowitz<sup>19</sup> to attribute any higher  $T_c$ 's observed in nonstoichiometric samples to surface effects. We have resumed the experimental investigations on  $\text{Rb}_x\text{WO}_3$ , also encouraged by the acknowledgment that interesting phenomena are often hidden behind poorly reproducible data.

A great part of our work had to deal with physical chemistry issues. It will be described in a forthcoming paper,<sup>20</sup> hereafter referred to as II.

## II. EXPERIMENT

### A. Preparation of samples

In the first stage of our investigations, we studied single crystals grown electrolytically from a melt consisting of  $\text{Rb}_2\text{CO}_3$  and  $\text{WO}_3$ —according to the method developed by Sienko and Morehouse.<sup>21</sup> Contrary to some authors who claimed to have obtained big single crystals with  $0.19 < x < 0.33$ , we had good results, by using this method, only for the stoichiometric ( $x \approx 0.33$ ) melt. Moreover, it was very difficult to guarantee that these crystals were completely free from occlusions of the melt. As our aim was first to clarify how the superconducting properties depend on  $x$ , we needed homogeneous samples and a good knowledge of their composition. Therefore, we preferred carrying out this study with powder samples that have been prepared by the usual solid-state reaction: for each nominal  $x$  value, the starting material was made up from high-purity  $\text{Rb}_2\text{WO}_4$ ,  $\text{WO}_3$ , and W that were ground together and placed in a quartz tube. Before the tube was sealed, the mixture was pumped to  $10^{-6}$  Torr and baked repeatedly at about  $150^\circ\text{C}$  until we observed no more outgassing. The tube was then heated at  $900^\circ\text{C}$  for 2 days.

As discussed in more detail in II, we found no benefit from increasing the temperature above  $900^\circ\text{C}$ , as we did not try to obtain single crystals; on the contrary, we observed that higher temperatures resulted in attack on the quartz by the rubidium escaping from the Rb-rich samples.

This procedure yields fine crystalline powders with grain sizes ranging between about 10 and 100  $\mu\text{m}$  (bigger crystals being found near the  $x \approx 0.33$  content). By checking that the x-ray powder diffraction patterns of these samples agree with the HTB symmetry, and display no trace of another phase, we can be quite confident in taking for  $x$  its nominal value. This has been confirmed by the microprobe analysis of some of the samples.

It should be noticed that a solid-state reaction cannot lead to a perfectly homogeneous nonstoichiometric compound: each crystal is poorly connected to its neighbors in a low-pressure vapor and should reach an equilibrium weakly depending on its morphology and neighborhood. From our microprobe analysis we estimate the dispersion of the Rb content in our batches at  $0.005 \leq \delta x \leq 0.01$ .

### B. Characterization of the superconducting transition

We used a mutual-inductance bridge and a standard  $^4\text{He}$  cryostat to systematically characterize the superconducting transition by monitoring the diamagnetic expulsion in a small, ( $< 2 \times 10^{-4}$  T) low-frequency (33 Hz) magnetic field. Magnetic susceptibility measurements in static fields were also done with a superconducting quantum interference device magnetometer. These methods are better suited to the investigations we were concerned with than conductivity measurements. The width of the magnetic transition gives a good picture of the homogeneity of the sample, whereas a zero-resistance state may be due only to minute superconducting sheets or filaments. Moreover, as we shall show later, a crystal that was grown from the vapor and has a suitable size for conductivity measurements may not be a representative of the nominal composition of the batch, whereas this can be checked readily on powder samples by taking them from different parts of the powder batch.

We also carried out magnetic susceptibility and conductivity measurements on various single crystals but these experiments—which will be discussed in due course—will not be included in our determination of the  $T_c$  vs  $x$  dependence.

The amplitude of the magnetic transition of the powder samples could vary on a rather large range ( $\pm 20\%$ ), but we determined that this was only related to the size and morphology of the grains as well as to the compactness of the samples.

## III. RESULTS

We tried to find out the cause(s) of the nonreproducibility of the superconducting transition temperature  $T_c$  by first looking for a phase transition between room temperature and  $900^\circ\text{C}$ . We used differential thermal analysis and differential scanning calorimetry (DSC), and tried to anneal and quench the samples from various temperatures but we found no sign of a phase transition. However, these heat treatments have brought to light some aspects of the physical chemistry of these compounds, which could explain a part of the discrepancies previously noticed. We shall deal with this in II and here we describe what appeared to be the major cause of these discrepancies: the  $T_c$  of the nonstoichiometric compounds is sensible to the cooling rate below the room temperature. This was the expected consequence of an ordering of the Rb vacancies like the one described by Sato *et al.*,<sup>9</sup> but we first missed this cooling-rate effect because we tried to detect it in the region of the composition range where the previously observed dispersion of  $T_c(x)$  was the highest, i.e., near  $x \approx 0.25$ . In this range, we never observed superconductivity above 1 K, contrary to what claimed by Stanley *et al.*<sup>11</sup>

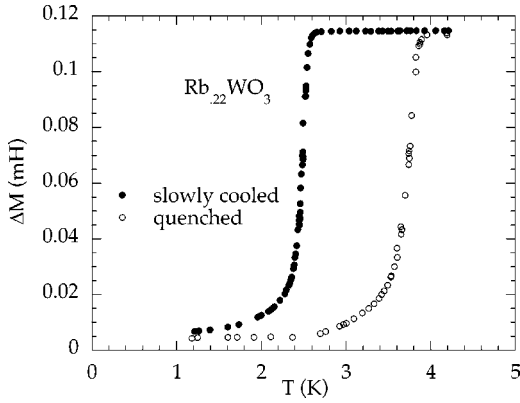


FIG. 1. Superconducting transitions (mutual-inductance variations) of a powder sample of  $\text{Rb}_{0.22}\text{WO}_3$  after different cooling rates.

### A. The cooling-rate effect

We have observed this effect for  $0.29 \leq x \leq 0.31$  and for  $0.19 \leq x \leq 0.23$ , and it is exemplified in Fig. 1: the “slowly cooled” sample has been cooled down to 90 K within a few hours before we transferred liquid helium; the same “quenched” sample reached 4.2 K within a couple of minutes after it has been introduced directly in the cryostat filled with liquid helium. As shown in Fig. 1, it is the “slowly cooled” samples that have a lower  $T_c$ , contrary to what is expected—and most usually observed—for a better ordered state. We also experimented with a faster cooling down to 90 K by dropping and stirring the sample in liquid nitrogen, but we observed no further increase in  $T_c$ . We also observed that the quenched state can be annealed at temperatures above  $T_m \approx (110 \pm 10)$  K and, in this respect, we saw no difference between the three samples studied with  $x = 0.19$ ,  $x = 0.22$  or  $x = 0.29$ .

The cooling-rate effect clearly confirms the ordering of the Rb atoms in the nonstoichiometric HTB and their extreme mobilities. We shall present now the other information we obtained on the order-disorder transformation.

### B. Calorimetric study of the order-disorder transformation

After several unsuccessful attempts, we finally observed the enthalpy anomaly accompanying this transformation, but

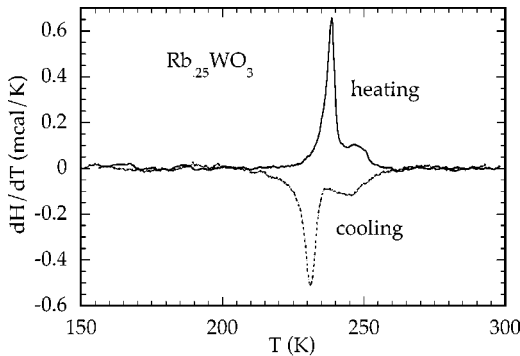


FIG. 2. DSC thermograms observed on a powder sample of  $\text{Rb}_{0.25}\text{WO}_3$  ( $\approx 50$  mg) on heating and on cooling at  $\pm 10$  K/min.

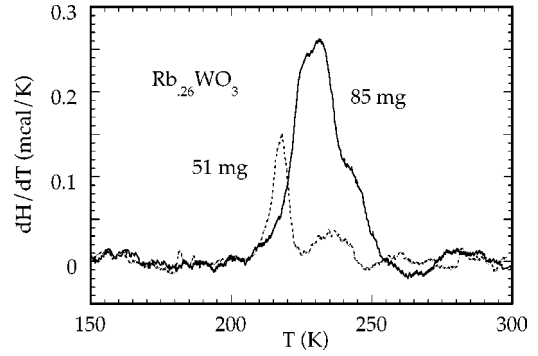


FIG. 3. DSC thermograms observed for two powder samples of  $\text{Rb}_{0.26}\text{WO}_3$  on heating (10 K/min).

only in the samples with  $x \approx 0.25$ . The apparatus we used was a Perkin-Elmer DSC-7 and our measurements extended down to  $\sim 100$  K. As the anomaly is quite weak, we had to use rather sizeable powder samples and high heating or cooling rates. This could partly explain the large temperature range of the anomaly and the thermal hysteresis, which are exemplified in Fig. 2. However, by comparing the behaviors of different samples, it appears that the width of the anomaly is mainly related to its strong  $x$  dependence and to the imperfect homogeneity of the samples. The data presented in Fig. 3 indicate that a composition difference  $\delta x \approx 0.01$  in the neighborhood of  $x = 0.25$  leads to a shift of the anomaly by about 20 K—the largest extrapolated peak onset temperature we observed being about 240 K.

Our results are rather in good agreement with those of Sato *et al.*,<sup>9</sup> however, we observed no anomaly for  $0.16 \leq x \leq 0.23$  and  $0.27 \leq x \leq 0.33$ , which shows that the transition is first order only for  $x$  in a narrow range around  $x = 0.25$ . Outside this range, the transition should become continuous and, actually, it is what is observed in the powder-diffraction pattern of  $\text{Rb}_{0.27}\text{WO}_3$ .

In our  $x \approx 0.25$  samples, we estimate the maximum heat absorption  $\Delta H$  that accompany the order-disorder transition to be  $80 \pm 10$  J/mol K, and the maximum entropy increase  $\Delta S$  to be  $0.35 \pm 0.05$  J/mol K. This value indicates that the degree of order in  $\text{Rb}_{0.25}\text{WO}_3$  is quite low just before it transforms into the high-temperature disordered state. Actually, the molar configurational entropy of the disordered state is then associated with the number of ways ( $w$ ) of arranging  $N$  rubidium vacancies over  $4N$  sites, i.e.,  $S_{\text{dis}} = k_B \ln w$ , with

$$w = \frac{N!}{\left(\frac{N}{4}\right)! \left(\frac{3N}{4}\right)!} \quad \text{and} \quad N = N_0/3,$$

as  $x = 0.25$  corresponds to 1/4 of the Rb atoms missing from the  $N_0/3$  sites per mole available in the HTB structure. It gives  $S_{\text{dis}} = 1.56$  J/mol K. If we eliminate all the arrangements where two vacancies or more are first neighbors we find that  $w$  should be

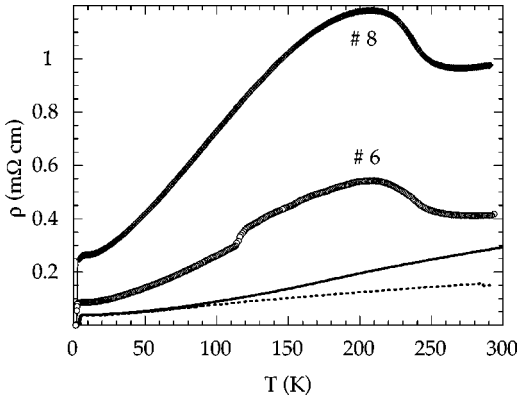


FIG. 4. Temperature dependence of the resistivity ( $\parallel c$ ) of two vapor-grown type-A fibers, compared with two massive acid-etched samples ( $x \approx 0.19$ ) cut ( $\perp c$ ) in an electrochemically grown crystal (full and dashed curves).

$$w = \frac{\left(\frac{3N}{4}\right)!}{\left(\frac{N}{4}\right)! \left(\frac{N}{2}\right)!},$$

which gives  $S_{\text{dis}} = 1.32$  J/mol K. Accordingly, the increase of entropy  $\Delta S$  that we observed at the first-order transition amounts to about 22–26% of  $S_{\text{dis}}$ . This is rather in good agreement with the simple Bragg-Williams approximation applied to  $AB_3$  alloys, which gives  $\Delta S/S_{\text{dis}} = 17.5\%$ .

### C. The resistivity anomaly

As mentioned earlier, Sato *et al.*<sup>9</sup> had noticed that the order-disorder transition temperature  $T_s$  that they determined from their neutron-diffraction data seemed to correspond to the temperature  $T_B$  of the resistivity anomaly observed by Stanley *et al.*<sup>11</sup> It was therefore very tempting to attribute this anomaly to the ordering of the Rb atoms. Since our results clearly confirmed this ordering and showed its strong effect on the stability of the superconducting state, it was still more difficult to understand why this resistivity anomaly had not been observed by other authors. This led us to undertake new resistivity measurements on single crystals obtained by following the same procedure as that of Stanley *et al.*,<sup>11</sup> i.e., a solid-state reaction at 950 °C for 5 days. In this way, we prepared about 5 g of  $\text{Rb}_{0.26}\text{WO}_3$  and obtained the usual poorly crystallized, partly sintered powder, plus a few milligrams of needlelike crystals. These often radiate in bundles from tiny crystals attached to the quartz surface; this shows that they grew from the vapor. Most of these needles were dark blue and displayed the hexagonal symmetry of the HTB, but we also observed light-blue whiskers and even transparent ones, some of which were curved and even spiraled. We selected some of the dark-blue needles, which were about 5 mm long in the  $c$ -axis direction and rather ribbon shaped, therefore, well suited to resistivity measurements (about 20–50  $\mu\text{m}$  in width and 2–5  $\mu\text{m}$  in thickness).

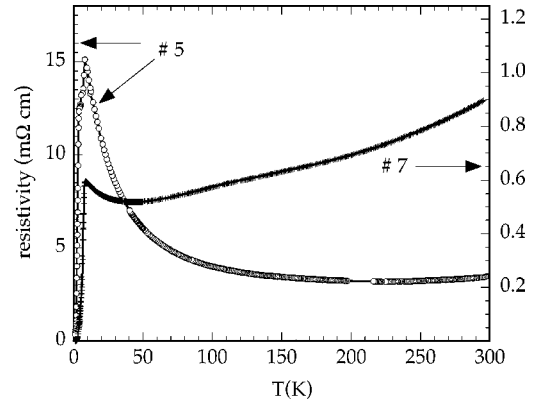


FIG. 5. Temperature dependence of the resistivity ( $\parallel c$ ) of two vapor-grown type-B fibers.

Silver or gold paints that are usually used to attach current and potential leads to small samples, do not give satisfactory electrical contacts on  $\text{Rb}_x\text{WO}_3$  even by using freshly prepared crystals. While evaporated coatings are not very effective, we obtained very good results by first sputtering gold on the contact areas. This nonconducting behavior of the sample surface will be considered in II. The device we used produces contact areas partly enveloping the samples, specially at their ends, which should allow fairly uniform current lines.

We measured the temperature dependence of the resistivity of seven of these samples between 300 K and 1.2 K, by using always slow cooling or heating rates (about 2 K/min) and we observed: (1) in two samples (A), an anomalous hump in the resistivity ( $\rho$ ) as a function of temperature (Fig. 4)—similar to the one observed by Stanley *et al.*,<sup>11</sup> (2) in the other samples (B), a low-temperature upturn of  $\rho$  (Fig. 5); (3) in all samples, a vanishing of  $\rho$  occurring between  $\approx 8$  K and  $\approx 2$  K (Fig. 6), whereas, as usual, no sign of superconductivity was detected in the magnetic susceptibility of the powder samples of the batch; and (4) large non-linear effects, in the same temperature range (see Sec. III D). These conflicting observations prompted us to question the

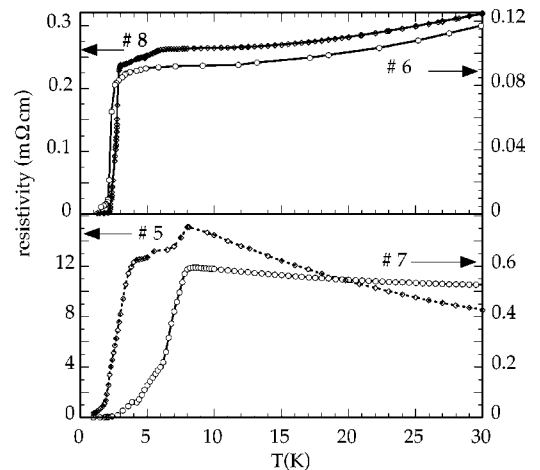


FIG. 6. Temperature dependence of the resistivity ( $\parallel c$ ) of the two types of vapor-grown fibers near the superconducting transition.



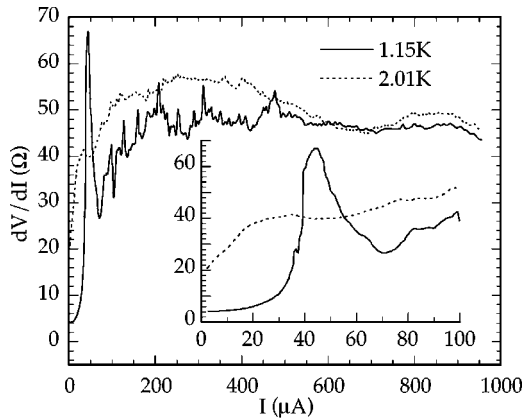


FIG. 7. Low-temperature differential resistance of the vapor-grown sample no. 5 as a function of the bias current. The inset magnifies the low-current range.

identity of these fibers and to carry out their examination with a JEOL 840-A scanning electron microscope (SEM) fitted with an energy dispersive spectrometer. This revealed that none of these vapor-transported crystals are really representative of  $\text{Rb}_{0.26}\text{WO}_3$ : their rubidium content are much higher than the nominal content of the batch, samples *B* being structurally and chemically more homogeneous. We suspect that the special transport properties of these fibers are the consequences of their structural nonhomogeneity that could affect microscopic as well as mesoscopic scales. We suggest that crystallization from the vapor might lead to the growth of rather decoupled layers of HTB sometimes with, possibly, really different Rb contents. Besides, each layer or strip might be often perturbed by extended defects. We shall discuss the possible nature of these interlayers and interlayer defects in II.

Within this framework, we propose the following description of the features listed above.

(1) The main decrease of the resistance—occurring at about 2.5 K in samples *A*—is probably associated with the superconducting transition of nearly stoichiometric  $\text{Rb}_{0.33}\text{WO}_3$  strips. But in some samples, and particularly in samples *B*, the resistance begins to decrease at about 8 K, which is much higher than the highest  $T_c$ 's ever observed in HTB via magnetic measurements (cf. Sec. III E). We are not dealing here with intrinsic superconductivity but rather with superficial or filamentary effects similar to those observed in  $\text{NbSe}_3$ ,<sup>22</sup> for instance.

(2) The low-temperature nonlinear conductivity is a symptom, which is related to the defects mentioned above.

#### D. The nonlinear resistivity behavior of the vapor-grown fibers

At temperatures below about 2 K, the differential resistance  $dV/di$  steeply rises when the bias current exceeds a critical value  $I_c$  and then decreases toward the value of the normal state resistance (Figs. 7 and 8). Sweeping the bias current up or down at different rates does not modify significantly the current dependence of  $dV/di$ , which is not very sensitive either to the thermal cycling. Well below and also

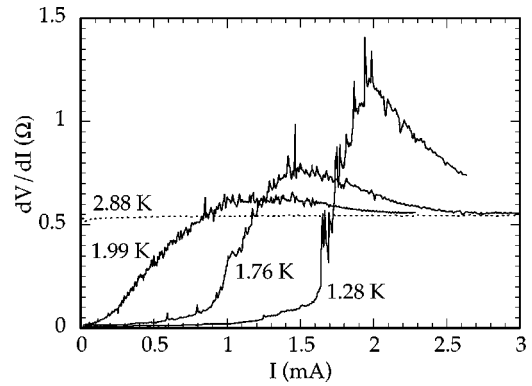


FIG. 8. Low-temperature differential resistance of the vapor-grown sample no. 6 as a function of the bias current.

beyond  $I_c$  the differential resistance displays rather erratic features that seem to be related to noise generating instabilities.

Assuming a uniform current distribution, the  $I_c$  values at  $\approx 1.2$  K would correspond to current densities  $j_c$  ranging between about  $0.05 \text{ A/mm}^2$  and  $20 \text{ A/mm}^2$ , depending on the samples. We found no correlation between this spread of the  $j_c$  values and the morphology of the samples or their apparent resistivities—which are also widely spread and significantly greater than that quoted in the literature: at 300 K they range between  $\approx 4 \times 10^{-4} \text{ } \Omega \text{ cm}$  and  $3.5 \times 10^{-3} \text{ } \Omega \text{ cm}$  whereas the published values stand between  $3 \times 10^{-5} \text{ } \Omega \text{ cm}$  and  $1.5 \times 10^{-4} \text{ } \Omega \text{ cm}$ .

We shall notice also that the nonohmic behavior is observed too, above 8 K, in the “normal” state of those samples that display the greatest resistivity upturn: where, at temperatures up to  $\approx 20$  K, increasing the bias current leads to a significant decrease in the resistance.

We think that these nonlinear effects originate from a distribution of weak links throughout the samples, which leads to complex tunneling effects; in particular, below  $\approx 2$  K, the features exemplified in Figs. 7 and 8 are quite reminiscent of those observed in granular materials and are attributed to the Josephson tunneling between the grains.<sup>23</sup> This picture is consistent with the high resistivity of these crystals and suggests that normal tunneling could be responsible for the nonohmicity displayed in the normal state below about 20 K.

We shall now sum up the information we have on the anomalous hump in the resistivity, which motivated this study. We only observed this hump in two of the seven vapor-grown samples and never observed it—whatever be the Rb content—in more massive crystals prepared by fused-salt electrolysis.<sup>24</sup> In these the resistivity decreases quite linearly with temperature down to about 100 K, before it progressively saturates (Fig. 4). This is also the behavior observed by Aristimúno *et al.*<sup>14</sup> in the crystals that were carefully selected to be electrically homogeneous. On the contrary, we showed that the vapor-grown crystals are not homogeneous and display a transition towards a zero-resistance state, which begins at about 8 K. This resistance anomaly is not observed magnetically in any bulk HTB. The foregoing remarks lead us to suspect that the resistivity anomaly is extrinsic and related to the inhomogeneity of the

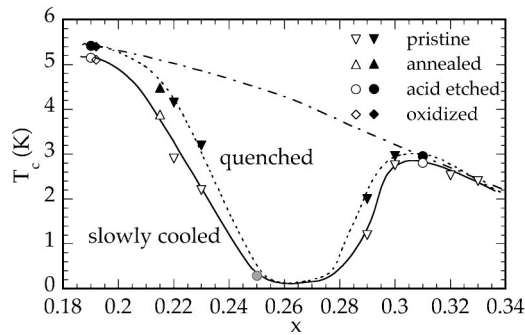


FIG. 9. The superconducting transition  $T_c$  as a function of the rubidium content  $x$ . Empty or full markers refer to measurements after slow cooling or quenching from  $\approx 300$  K, respectively. The grey marker corresponds to an intermediary cooling in a  $^3\text{He}$ - $^4\text{He}$  dilution refrigerator. The curves are only guides to the eye and the monotonous one extrapolates what we think would be the  $T_c(x)$  dependence if the vacancy ordering could be prevented.

samples. However, its occurrence in the same temperature range as the order-disorder transition is certainly not merely a matter of chance. Actually the same Florida State University group observed the same anomalies in  $\text{K}_x\text{WO}_3$ ,<sup>12</sup> but at higher temperatures, and no anomaly in  $\text{Cs}_x\text{WO}_3$  (Ref. 13)—which is consistent with the greater tendency for the smaller ions to order. As described below, this also agrees with the quite different  $T_c(x)$  dependences observed in the three bronzes. The only explanation we can offer to rationalize these behaviors is the following: the ordering of the Rb atoms leads to a reduction of the density of states at the Fermi level  $D_{\text{FE}}$ , which destabilizes the superconducting state but has only a minute effect on the resistivity of the normal state in the massive samples.<sup>25</sup> On the other hand, in the vapor-grown samples, the loss of conductivity associated with the structural defects—those revealed by the nonlinear effects described above—could be enhanced by the reduction of  $D_{\text{FE}}$  and could lead to the hump observed.

### E. The $T_c(x)$ phase diagram

The information collected above confirms that we should not rely on the composition of the vapor-grown samples to establish the tungsten bronze  $T_c(x)$  phase diagram. It also allows us to dismiss the high values of  $T_c$  observed by Stanley *et al.*<sup>11</sup> near  $x=0.25$ . As we just saw, they are probably to be ascribed to a kind of filamentary superconductivity, whereas the  $T_c$ 's of the corresponding bulk material deeply decrease—as a result of the ordering of the Rb vacancies. The  $x$  dependence of  $T_c$  therefore displays a pronounced dip near this Rb content which allows the greatest degree of order and leads to the highest transformation temperature  $T_{\text{ord}}$  (Fig. 9). This dip is less pronounced when the samples are quenched from room temperature but ordinary quenching rates are not sufficient to prevent a significant ordering when  $0.23 \leq x \leq 0.28$ , and superconductivity cannot develop above  $\approx 1$  K within this composition range. Beyond this range,  $T_c$  steeply increases with  $x$  up to  $T_c \approx 3$  K for  $x \approx 0.30$ , and then slowly decreases down to  $T_c \approx 2$  K, when the Rb content approaches the stoichiometric value. On the other side of the

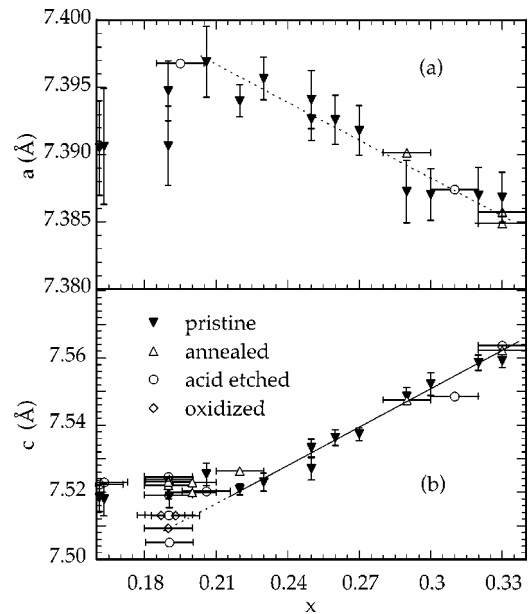


FIG. 10. Dependence of the lattice parameters of the HTB phase as a function of the rubidium content. Nominal  $x$  values are used for the pristine samples whereas the mean values deduced from the SEM analysis are used for the other samples. Below  $x \approx 0.20$ , most of the data for the  $a$  parameter have been omitted because of their very poor accuracy—probably due to the blurring effect of the parasitic phase.

dip,  $T_c$  increases still more abruptly with the decrease of the Rb content and seems to level off at  $T_c \approx 5$  K for  $x \leq 0.21$ . However, this asymptotic behavior seems to conflict with the higher  $T_c$ 's ( $\approx 5.5$  K) that we can obtain in the samples in which the Rb content has been reduced by acid etching or by a slight oxidation.<sup>26</sup>

This inconsistency prompted us to question the stability of the HTB phase for  $x \leq 0.22$ . By examining more systematically the x-ray powder patterns, we found that the  $x$  dependence of the lattice parameters shows a discontinuity near  $x \approx 0.215 \pm 0.005$  in samples prepared by the usual solid-state reaction method (Fig. 10). This clearly indicates that another phase coexists with the HTB's when the rubidium content falls below this value. In the slowly cooled samples, the corresponding diffraction peaks begin to appear unambiguously only when  $x \leq 0.19$ , a value which was therefore associated, until now, with the boundary of the HTB-phase region. In these samples, we found that  $\text{WO}_3$  coexists with the HTB phase and gives hardly perceptible diffraction peaks—which agree with the fact that  $\text{Rb}_{0.21}\text{WO}_3$  should be in equilibrium with only about 10% of  $\text{WO}_3$  when the nominal Rb/W ratio is 0.19. In samples that were quenched at the end of their otherwise similar preparative treatment, the larger additional peaks can be attributed to the intergrowth tungsten bronzes (ITB) phases and seem compatible with a content amounting to 20%. These observations are consistent with an ITB- $\text{WO}_3$  boundary situated near  $700^\circ\text{C}$ – $800^\circ\text{C}$ , as proposed by Hussain.<sup>27</sup>

On the other hand, the acid-etched or slightly oxidized samples in which we observed the highest  $T_c$ 's, display also the lowest  $c$ -parameter values. Moreover, these values corre-

spond to what is expected for an HTB phase with  $0.19 \leq x \leq 0.20$ —extending the linear decrease of  $c$  with  $x$  observed at higher Rb contents (see Fig. 10).<sup>28</sup> Correspondingly, we think that the superconducting transitions that begin above 5 K in the latter samples are to be attributed to this structure and to the rubidium content.

This led us to complete the low- $x$  region of  $T_c(x)$  diagram as displayed in Fig. 9. The transition temperature  $T_c$  has been defined here at the onset of the diamagnetic expulsion, as the width of the transition considerably depends on the samples: it can be only about 0.2 K in nearly stoichiometric samples ( $x \leq 0.30$ ) that are less sensitive to the ordering transformation, but it can be more than 1 K when the Rb content of the samples leads to the stronger cooling-rate effect. We also observed that the powder samples with  $x \leq 0.23$ , which were annealed at 950 °C and partly sintered, displayed much steeper transitions, but they recover their pristine behavior when they were powdered again. This probably indicates that the penetration depth  $\lambda$  in these samples is close to the size of a notable proportion of the grains, i.e., of the order of at least 1  $\mu\text{m}$ .

Although at first sight it looks quite different, this  $T_c(x)$  diagram cannot but recall the corresponding  $\text{Cs}_x\text{WO}_3$  diagram that displays a monotonic increase of  $T_c$  with decreasing  $x$ . Actually, the strong reduction of  $T_c$  near  $x \approx 0.25$  in  $\text{Rb}_x\text{WO}_3$  is the signature of the rubidium vacancies ordering. This effect is still more pronounced in  $\text{K}_x\text{WO}_3$ —where the ordering is very easy<sup>10</sup>—whereas it is absent in the cesium tungsten bronze, where no noticeable ordering seems to occur. In other words, the  $T_c(x)$  diagrams of the potassium and rubidium hexagonal tungsten bronzes would be quite similar to the diagram of  $\text{Cs}_x\text{WO}_3$ , if we could prevent the smaller alkali ions from ordering. Finally, we shall notice that the  $x$  dependences we obtained for the lattice parameters in  $\text{Rb}_x\text{WO}_3$ —as displayed in Fig. 10—are now quite similar to the corresponding ones in  $\text{Cs}_x\text{WO}_3$ :<sup>29</sup> the decrease of the alkali-metal content leads to a decrease of the  $c/a$  ratio; the larger alkali metals giving the larger effect and, probably, playing a more effective role in the stabilization of the HTB phase, as indicated by the fact that they lead to a farther extended homogeneity range, on its low- $x$  side.

## IV. DISCUSSION

### A. The $T_c(x)$ issue

We shall first remark that this increase of  $T_c$  with decreasing  $x$  was also observed in the TTB  $\text{Na}_x\text{WO}_3$  and  $\text{K}_x\text{WO}_3$ .<sup>30</sup> Well before the discovery of the high- $T_c$  cuprates this behavior aroused a great interest. The point is that it seems to conflict with the simple BCS model because a decrease of the alkali content should correspond to a decrease of the density of state at the Fermi level  $\mathcal{D}_{\text{FE}}$ . This has been well established in the case of the most extensively studied tungsten bronze  $\text{Na}_x\text{WO}_3$ .<sup>31,32</sup> The increase in  $T_c$  with decreasing  $x$  in these compounds is therefore probably due to an enhancement of the electron-electron interaction in the low- $x$  range. Although we have less clues to support this diagnosis

as far as  $\text{Rb}_x\text{WO}_3$  is concerned,<sup>33</sup> we think it remains the most likely in view of the various analogies between the two systems.

Salchow *et al.*<sup>34</sup> attributed the increase in  $T_c$  with increasing  $x$  to a better screening of the electron-phonon interaction. We think that this mechanism is probably not very effective in the HTB, because it would imply that the ordering of the alkali vacancies—which certainly reduces  $\mathcal{D}_{\text{FE}}$ —would increase  $T_c$ , whereas it is drastically reduced. Another mediation of the electron-electron interaction has been proposed by Kahn and Ruvalds<sup>35</sup> who invoked acoustic plasmons but, at the moment, we consider that the reliable experimental data on these bronzes are in favor of those models that rely on the lattice instability.

Actually the crystal structure of these bronzes is not very stable: according to Sato *et al.*,<sup>9</sup> a distortion of the  $\text{WO}_3$  cage takes place in  $\text{Rb}_x\text{WO}_3$  below about 420 K. Above this transition the space group is  $P6_3/mcm$ , but below this temperature the exact structure remained unsolved at that time. A similar poor agreement with any structural model is observed in  $\text{K}_x\text{WO}_3$ .<sup>10,36</sup> Most of these studies indicate that the topology of the oxygen octahedra is disturbed around an alkali vacancy. Moreover, the great versatility of these octahedra is well known: they are able to join along different directions by sharing their corners, or even their edges, and to yield to various deformations—which makes the structures they form able to sustain large deviations from stoichiometry. This leads to the spectacular “crystallographic shear” planes in  $\text{WO}_{3-x}$ , to the lamellar intergrowth of HTB and  $\text{WO}_3$  in low-alkali-content ITB’s and to many  $\text{WO}_6$ -based metastable structures formed at rather low temperatures, via the methods of soft chemistry.

On the other hand, we have many evidences of the great mobility of the small alkali atoms in the tungsten bronzes. In the HTB, particularly, low-frequency Einstein-like phonon modes are associated to the vibrations of these atoms within the large channels running along the  $c$  direction.<sup>37</sup> These modes were made responsible for the “excess” heat capacity observed above about 10 K, and which can be fitted—in  $\text{Rb}_{0.33}\text{WO}_3$ —by an Einstein contribution with  $\Theta_E \approx 60$  K.<sup>18</sup> However, as their characteristic energy seems to hardly depend on  $x$ ,<sup>9</sup> they probably are not the main cause for the anomalous  $T_c(x)$  dependence.

Other special phonons have been invoked, originally by Shanks,<sup>2</sup> and have given rise to the local structural excitation (LSE) model proposed by Ngai and Silbergliitt,<sup>38</sup> and then treated by Vujičić *et al.*<sup>39</sup> They attribute the enhancement of the electron-electron attractive interaction in the tungsten bronzes to local structural instabilities: their model is based on the idea that a local ground-state configuration could be separated from one or more configurations by a small amount of energy and by a potential barrier. According to these authors, the excitations between these local states—which they called LSE’s—could not only enhance the phonon pairing of electrons but also mediate a supplementary effective electron-electron interaction through a specific electron-LSE interaction.

One of the strong points of this model lies in the fact that the local structural instabilities are associated with the alkali



vacancies and it is conceivable that increasing their content should increase the instability of the lattice and the part of the LSE in its dynamics, whereas the ordering of these vacancies should have the opposite effect. Following the approach of Ngai and Silbergliitt,<sup>38</sup> we may imagine, in the case of  $\text{Rb}_x\text{WO}_3$ , that there are microscopic regions where the local density  $x_l$  is smaller than the average value  $x$  and thus where there is a tendency, for the  $\text{WO}_6$  octahedra, to collapse into a  $\text{WO}_3$  structure—which reminds us of the intergrowth mechanism leading to the ITB phases when  $x \leq 0.2$ . Where a local transformation has occurred, a kind of  $\text{WO}_3$  defect has been formed. On the other hand, if the local transformation has not condensed, the local structural instability is preserved, and the elemental  $\text{WO}_3$  defect can be viewed as an excited state of the local group of atoms and bonds. Finally, it is also tempting to speculate that the large amplitude vibrations of the alkali atoms could facilitate the tunneling between the free-energy minima of two structural configurations or, more generally, that combinations of these local instabilities with the alkali-atom vibrations could lead to a specially effective coupling with the conduction electrons.

The LSE model has been adopted by Sato *et al.*<sup>9</sup> and applied to  $\text{Rb}_x\text{WO}_3$  by using the McMillan's equation<sup>40</sup> where they introduced an electron-phonon coupling parameter  $\lambda_{\text{LSE}}$  proportional to  $n_{\text{LSE}}$ —the number of LSE—and to  $\mathcal{D}_{\text{FE}}$ . This simple approach is able to describe the  $x$  dependence of  $T_c$  as it provides the necessary increase of  $\lambda$  with the decrease of  $x$ . However, the inelastic neutron scattering experiments undertaken by these authors on powder samples have not allowed to observe any significant  $x$  dependence. As proposed by these authors, a tentative explanation of this failure could lie in the broadness of the LSE spectrum; however that may be, and this issue deserves to be experimentally settled.

### B. Interfacial superconductivity

Besides this problematic  $T_c(x)$  dependence, superconductivity in  $\text{Rb}_x\text{WO}_3$  displays another unusual feature that has been revealed by our resistivity measurements on the vapor-transported samples, namely, its stabilization—at temperatures above the highest  $T_c$ 's of the bulk material—in probably interfacial regions. Such a phenomenon has been observed in  $\text{WO}_{3-x}$ ,<sup>4</sup> and attributed to twin walls. Sheet superconductivity also develops on the surface of  $\text{WO}_3$  crystals that have been subjected to a slight superficial enrichment of sodium.<sup>5</sup> The very high  $T_c$ 's observed in the latter case (up to 91 K) is evidently far from being explained but indicates how much the interfacial properties of these materials could be promising. The great versatility of the  $\text{WO}_6$  octahedra we discussed above, certainly plays a part in these superficial or interfacial properties.

An explanation of such enhancements of  $T_c$  was proposed, twenty five years ago, by Lefkowitz,<sup>19</sup> who thought that the anomalous  $T_c(x)$  dependence in the tungsten bronzes was a surface effect: he stressed that a ferroelectric instability can condense at low temperatures in  $\text{WO}_3$  and hypothesized that this could lead to high electric fields at the boundary between the insulating material and the doped regions—thus inducing a new electron density of states at the

Fermi level. Although we are now quite sure that the increase in  $T_c$  with the reduction of the alkali content in these bronzes is really a bulk property, the Lefkowitz's proposition seems fairly seductive when considering the phenomenon we observed in the vapor-transported samples.

### C. The order-disorder transformation

Finally, we shall add a few comments about the order-disorder transition of the rubidium vacancies in  $\text{Rb}_x\text{WO}_3$ . It was observed first by the neutron-diffraction measurements<sup>9</sup> and then by the electron-diffraction measurements.<sup>41</sup> Our calorimetric measurements have shown that this transformation was first order only for  $x \approx 0.25$ , which corresponds to one-quarter of the Rb atoms being absent, to the most stable ordering and to a doubling of the lattice constants. It appears that the positions of the O atoms are modulated to some extent by the alkali vacancies,<sup>42</sup> therefore a gap at the Fermi surface is certainly induced by this new periodicity. Subsequently, the  $K$  ordering in  $\text{K}_x\text{WO}_3$  was also studied<sup>43</sup> and different ordering schemes have been proposed. A quite complex picture emerges from these studies, which indicates, one more time,<sup>44</sup> that we are dealing with an “infinitely adaptive structure.”

When we move away from  $x \approx 0.25$ , the transition temperature  $T_{\text{ord}}$  rapidly decreases: it is only about 200 K in  $\text{Rb}_{0.22}\text{WO}_3$  (Ref. 9) and about 123 K in  $\text{Rb}_{0.20}\text{WO}_3$ ,<sup>41</sup> i.e., very near from our estimate of the rubidium mobility threshold  $T_m$ , and this agrees with our observation that the disordered state, then, can be quenched more effectively. Conversely, the low-temperature state will be usually less ordered. Moreover, the complex ordering taking place when  $x < 0.25$  has probably a weaker effect on the Fermi surface. Therefore, both mechanisms contribute to reduce the cooling-rate effect when  $x$  approaches its minimum value.

Let us finally notice that similar issues, concerning order-disorder phenomena and their influence on superconductivity, have been raised in the high- $T_c$  cuprates.<sup>45</sup> A thermodynamical model for the ordering schemes of the oxygen vacancies has been proposed,<sup>46</sup> which leads to a concentration dependence of the ordering temperature quite reminiscent of the  $T_{\text{ord}}(x)$  behavior observed in  $\text{Rb}_x\text{WO}_3$ ; in particular, a first-order transition is predicted only in a part of the concentration range. However, ordering increases  $T_c$  in these cuprates as well as in the low- $T_c$  organic superconductors, whereas it is just the opposite in the HTB.

## V. CONCLUSION

We have identified the main reasons why the available results on the physical properties of the HTB  $\text{M}_x\text{WO}_3$  were so contradictory. We have described here the effect of the order-disorder transition and interface-related artifacts; other causes of discrepancies result from the physical chemistry of these compounds and will be described in the forthcoming paper II. We now have a much clearer vision of the HTB, which brings to the fore a common unusual feature of the superconducting state whose critical temperature  $T_c$  increases when the  $M$  content  $x$  and  $\mathcal{D}_{\text{FE}}$  decrease. This behav-



ior is also shared by the tetragonal tungsten bronze  $\text{Na}_x\text{WO}_3$ . After reviewing the reliable available information on these systems we concluded that a strong-coupling mechanism was probably responsible for this feature. At this respect, the model appealing to local LSE's seems the most attractive, and it is backed up by our observations that the superconducting state is destabilized by the ordering of the  $M$  vacancies, whereas  $T_c$  increases with their number. Actually, it is the only model, till now, which is able to conciliate these two features. However, we established that superconductivity is nearly completely suppressed in the HTB when 1/4 of the  $M$  atoms are missing and ordered, and this cannot be due only to the LSE mechanism as superconductivity exists up to  $\sim 2$  K in the stoichiometric HTB. Thus, the  $M$ -atom ordering also has a deep effect on the Fermi surface—in contradiction with the previous rigid-band descriptions. Conversely, this indicates that the strong-coupling LSE mechanism—if present—must be the most effective when  $T_c$  is the highest and  $\mathcal{D}_{\text{FE}}$  is simultaneously reduced by the

highest vacancy content and by their ordering, i.e., for  $x = 0.19$ . It is, therefore, near this concentration that more extensive lattice-dynamics studies should be carried out. More generally, from a fundamental point of view and irrespective of the quest for room-temperature superconductivity, we think that the possible building up of an attractive electron-electron coupling via localized interactions should be investigated most seriously and that  $\text{Rb}_x\text{WO}_3$  is now a system where this task may be tackled profitably.

#### ACKNOWLEDGMENTS

We are grateful to A. Sulpice for his magnetization measurements and to Y. Monfort for communication of unpublished data. We greatly acknowledge stimulating discussions with O. Béthoux and the assistance of P. Amiot and A. Hadj-Azzem in the x-ray powder-diffraction measurements and SEM examinations and analysis.

- <sup>1</sup>C.J. Raub, A.R. Sweedler, M.A. Jensen, S. Broadston, and B.T. Matthias, *Phys. Rev. Lett.* **13**, 746 (1964).
- <sup>2</sup>H.R. Shanks, *Solid State Commun.* **15**, 753 (1974).
- <sup>3</sup> $T_c$  as high as 7.7 K have been claimed by A.R. Sweedler, Ph.D. thesis, University of California, San Diego, 1969 (unpublished); see also Stanley *et al.* (Ref. 11).
- <sup>4</sup>A. Aird and E.K.H. Salje, *J. Phys.: Condens. Matter* **10**, L377 (1998); A. Aird, M.C. Domeneghetti, F. Mazzi, V. Tazzoli, and E.K.H. Salje, *ibid.* **10**, L569 (1998).
- <sup>5</sup>S. Reich and Y. Tsabba, *Eur. Phys. J. B* **9**, 1 (1999); Y. Levy, O. Millo, A. Sharoni, Y. Tsabba, G. Leitus, and S. Reich, *Europhys. Lett.* **51**, 564 (2000).
- <sup>6</sup>A. Magnéli, *Acta Chem. Scand.* (1947-1973) **7**, 315 (1953).
- <sup>7</sup>A. Hjelm, C.G. Granqvist, and J.M. Wills, *Phys. Rev. B* **54**, 2436 (1996).
- <sup>8</sup>H. Höchst, R.D. Bringans, and H.R. Shanks, *Phys. Rev. B* **26**, 1702 (1982).
- <sup>9</sup>M. Sato, B.H. Grier, G. Shirane, and H. Fujishita, *Phys. Rev. B* **25**, 501 (1982); M. Sato, B.H. Grier, G. Shirane, and T. Akahane, *Phys. Rev. B* **25**, 6876 (1982); M. Sato, B.H. Grier, H. Fujishita, S. Hoshino, and A.R. Moodenbaugh, *J. Phys. C* **16**, 5217 (1983).
- <sup>10</sup>H.B. Krause, R. Vincent, and J.W. Steeds, *Solid State Commun.* **68**, 937 (1988); A.J. Schultz, H. Horiuchi, H.B. Krause, *Acta Crystallogr., Sect. C: Cryst. Struct. Commun.* **42**, 641 (1986).
- <sup>11</sup>R.K. Stanley, R.C. Morris, and W.G. Moulton, *Phys. Rev. B* **20**, 1903 (1979).
- <sup>12</sup>L.H. Cadwell, R.C. Morris, and W.G. Moulton, *Phys. Rev. B* **23**, 2219 (1981).
- <sup>13</sup>M.R. Skokan, W.G. Moulton, and R.C. Morris, *Phys. Rev. B* **20**, 3670 (1979).
- <sup>14</sup>A.R. Aristimúno, H.R. Shanks, and G.C. Danielson, *J. Solid State Chem.* **32**, 245 (1980).
- <sup>15</sup>J.P. Remeika, T.H. Geballe, B.T. Matthias, A.S. Cooper, G.W. Hull, and E.M. Kelly, *Phys. Lett.* **24A**, 565 (1967).
- <sup>16</sup>D.R. Wanlass and M.J. Sienko, *J. Solid State Chem.* **12**, 362 (1975).
- <sup>17</sup>C.N. King, J.A. Benda, R.L. Greene, and T.H. Geballe, in *Proceedings of the Thirteenth International Conference on Low Temperature Physics, Boulder, Colorado, 1972*, edited by R.H. Kropschot and K.D. Timmerhaus (University of Colorado Press, Boulder, Colorado, 1973).
- <sup>18</sup>A.J. Bevolo, H.R. Shanks, P.H. Slides, and G.C. Danielson, *Phys. Rev. B* **9**, 3220 (1974).
- <sup>19</sup>I. Lefkowitz, *Ferroelectrics* **16**, 239 (1977).
- <sup>20</sup>R. Brusetti and J. Marcus (unpublished).
- <sup>21</sup>M.J. Sienko and S.M. Morehouse, *Inorg. Chem.* **2**, 485 (1963).
- <sup>22</sup>K. Kawabata and M. Ido, *Solid State Commun.* **33**, 1539 (1982).
- <sup>23</sup>D.U. Gubser, S.A. Wolf, W.W. Fuller, and T.L. Francavilla, *Physica B & C* **107**, 485 (1981).
- <sup>24</sup>We have prepared some nonstoichiometric crystals by annealing stoichiometric electrocrystallized crystals within a large sample of compacted nonstoichiometric powder, or by acid etching (see II).
- <sup>25</sup>Resistivity measurements are not always able to detect rather large changes in  $\mathcal{D}_{\text{FE}}$ , as for instance in  $(\text{TMTSF})_2\text{ClO}_4$  [D.U. Gubser, W.W. Fuller, T.O. Poehler, J. Stokes, D.O. Cowan, M. Lee, and A.N. Block, *Mol. Cryst. Liq. Cryst.* **79**, 225 (1982)], and  $\text{Ti}_2\text{Mo}_6\text{Se}_6$  [R. Brusetti, A. Briggs, O. Laborde, M. Potel, and P. Gougeon, *Phys. Rev. B* **49**, 8931 (1994)].
- <sup>26</sup>It was known for a long time that acid etching could remove the Rb ions from the HTB and considerably enhance  $T_c$ . (Refs. 15–17). We have investigated this effect and we propose a description of the chemical process described in II. There we also describe how a moderate oxidation, at about 450 °C, can have a similar effect on the sample core, by driving the Rb ions towards the superficial tungstate layer.
- <sup>27</sup>A. Hussain, *Acta Chem. Scand., Ser. A* **32**, 479 (1978).
- <sup>28</sup>The corresponding increase of the  $a$  parameter is more difficult to bring to the fore because it is about four times smaller. Moreover, in the oxidized samples it is somewhat obscured by the

- presence of tungstate diffraction peaks.
- <sup>29</sup>The decrease in the  $c$ -axis lattice constant with decreasing rubidium concentration and the corresponding slight increase of  $a$  dimension was already observed by Hussain (Ref. 27) and by Wanlass and Sienko (Ref. 16). Our results are in better quantitative agreement with the latter ones. Shanks and Danielson referred to an opposite dependence of the  $c$  dimension, from which they extrapolate the  $x$  values in their samples prepared by the electrolytic method [H.R. Shanks and G.C. Danielson, in *Proceeding of the Twelfth International Conference on Low Temperature Physics, Kyoto, Japan*, edited by E. Kanda (Academic Press, New York, 1970), p. 359].
- <sup>30</sup>Unpublished data quoted by Ngai and Reinecke (1978), Ref. 38; see also Ref. 2.
- <sup>31</sup>M.J. Sienko, *Adv. Chem. Ser.* **39**, 224 (1963).
- <sup>32</sup>Experimental evidences (specific heat and photoemission spectroscopy) and band-structure calculations are discussed in Ref. 38, for instance.
- <sup>33</sup>In the case of  $\text{Rb}_x\text{WO}_3$ , we have only rough estimates of  $\mathcal{D}_{\text{FE}}$ : one can be derived from the Pauli-Peierls-type contribution to the magnetic susceptibility (Ref. 16), i.e.,  $\mathcal{D}_{\text{FE}} \approx 0.3$  state/eV mol—with no sensible variation with  $x$ —and another is provided by the thermodynamical properties of the superconducting state (Ref. 18), i.e.,  $\mathcal{D}_{\text{FE}} \approx 0.7$  state/eV mol in  $\text{Rb}_{0.33}\text{WO}_3$ . These estimates are quite similar to the values obtained in  $\text{Na}_x\text{WO}_3$  and, in both cases, are compatible with what can be expected from a nearly free electron band, accommodating the electrons donated by the alkali atoms.
- <sup>34</sup>R. Salchow, R. Liebmann, and J. Appel, *J. Phys. Chem. Solids* **44**, 245 (1983); *Solid State Commun.* **47**, 727 (1983).
- <sup>35</sup>L.M. Kahn and J. Ruvalds, *Phys. Rev. B* **19**, 5652 (1979); J. Ruvalds and L.M. Kahn, *J. Phys. (Paris)* **39**, C6 (1978).
- <sup>36</sup>M.F. Pye and P.G. Dickens, *Mater. Res. Bull.* **14**, 1397 (1979).
- <sup>37</sup>N.J. Chesser, J.G. Traylor, H.R. Shanks, and S.K. Sinha, *Ferroelectrics* **16**, 115 (1977); W.A. Kamitakahara, K. Scharnberg, and H.R. Shanks, *Phys. Rev. Lett.* **43**, 1607 (1979); see also Ref. 18.
- <sup>38</sup>K.L. Ngai and R. Silberglitt, *Phys. Rev. B* **13**, 1032 (1976); K.L. Ngai and T.L. Reinecke, *ibid.* **16**, 1077 (1977); *J. Phys. F: Met. Phys.* **8**, 151 (1978).
- <sup>39</sup>G.M. Vujičić, V.L. Aksenov, N.M. Plakida, and S. Stamenković, *J. Phys. C* **14**, 2377 (1981).
- <sup>40</sup>W.L. McMillan, *Phys. Rev.* **167**, 331 (1968).
- <sup>41</sup>Y. Monfort, P. Labbé, M. Goreaud, and G. Allais (unpublished); P. Labbé, *Key Eng. Mater.* **68**, 293 (1992).
- <sup>42</sup>See Schultz *et al.* in Ref. 10 and Sato *et al.* (1983) in Ref. 9.
- <sup>43</sup>H.B. Krause, W.G. Moulton, and R.C. Morris, *Acta Crystallogr., Sect. B: Struct. Sci.* **41**, 11 (1985); see also Ref. 10.
- <sup>44</sup>L. Kihlborg, M. Fernandez, Y. Laligant, and M. Sundberg, *Chem. Scr.* **28**, 71 (1988).
- <sup>45</sup>B.W. Veal, H. You, A.P. Paulikas, H. Shi, Y. Fang, and J.W. Downey, *Phys. Rev. B* **42**, 4770 (1990).
- <sup>46</sup>D. de Fontaine, G. Ceder, and M. Asta, *J. Less-Common Met.* **164&165**, 108 (1990).